



Thermal expander



Junying Huang^{a,b,*}, Xiangying Shen^{a,b}, Chaoran Jiang^{a,b}, Zuhui Wu^{a,b}, Jiping Huang^{a,b,*}

^a Department of Physics, State Key Laboratory of Surface Physics, and Key Laboratory of Micro and Nano Photonic Structures (MOE), Fudan University, Shanghai 200433, China

^b Collaborative Innovation Center of Advanced Microstructures, Nanjing 210093, China

ARTICLE INFO

Keywords:

Thermal expander
Heat flow
Efficient expanding effect
Efficient point-to-line conversion

ABSTRACT

One type of thermal device, named as thermal expander, is proposed and verified through both simulation and experiment. The thermal expander performs an efficient way to expand a heat flow of line-shape front. Moreover, the thermal expander shows an advantage in rectifying a heat flow from crooked front to line-shape front, which indicates that the thermal expander could act as an efficient point-to-line heat source convertor. We suggest that the thermal expander would be of help to energy saving and emission reduction, especially in thermal circuits and thermal management.

1. Introduction

As one of the fundamental energy transport phenomena in nature, heat flow automatically balances the thermal distribution around us [1]. Unfortunately, although people have realized that the ability to precisely control heat conduction will lead to an abundant wealth of applications (for example, thermal computation [2] and thermal memory [3]), heat flow management is still in its infancy [4–6]. To date, many interesting thermal devices (such as thermal rectifiers [6,7], thermal diodes [8–12], thermal cloaks [12–23], and so on [2,20,24–29]) have been proposed for the purpose of taming heat flow.

In experiments, these thermal devices are usually demonstrated with large scale heat flows of line-shape front (described by the shape of isothermal line) [12,15–18,20]. In order to realize a large heat flow of line-shape front, a heat source which is much larger than the sample size is always adopted [12,15,16]. Obviously, this method is not so efficient for the purpose of energy saving and emission reduction. Then comes a question: could we efficiently realize a large heat flow of line-shape front with a small heat source (heat flow) or even a point heat source?

Here, we propose a two-component thermal device, named as thermal expander. The thermal expander is realized by matching the thermal conductivities and geometries of two materials with a constraint condition. The thermal expander performs an efficient way to expand the heat flow of line-shape front, which is demonstrated through both simulation and experiment. Moreover, the thermal expander shows an advantage in rectifying a heat flow from crooked front to line-shape front, which is also verified by simulation and

experiment. We suggest that the thermal expander would be of help to energy saving and emission reduction, especially in thermal circuits and thermal management.

2. Theory

The thermal expander, schematically illustrated by red dashed lines in Fig. 1a, is composed of two symmetrical quarter rings (Material I) with the same inner radius R_1 and outer radius R_2 and with the thermal conductivity of κ_1 . The thermal conductivity of the connection (Material II) area between two quarter rings is κ_2 .

The condition for the efficient expanding effect of thermal expander on a heat flow of line-shape front is easy to figure out as: the front of heat flow on the end-position of the thermal expander (as indicated by red-arrow in Fig. 1b and 1c, respectively) must still be line-shape. To satisfy this condition, the front of heat flow in the area of Material II is kept to be line-shape (as shown in Fig. 1b). Therefore, the conduction equation should hold the form as the one dimensional Laplace equation (temperature distributions is a linear function of positions), that is, the shape of the material must have no effect on temperature distribution. Without loss of generality, for a polar coordinate system (r, θ) , considering two-dimensional thermal conduction equation for the steady state without the heat source and suppose all the materials involved are homogenous and isotropic, the dominant equation can be written as

$$\frac{1}{r} \frac{\partial}{\partial r} \left(r \frac{\partial T}{\partial r} \right) + \frac{1}{r^2} \frac{\partial^2 T}{\partial \theta^2} = 0, \quad (1)$$

* Corresponding authors at: Department of Physics, State Key Laboratory of Surface Physics, and Key Laboratory of Micro and Nano Photonic Structures (MOE), Fudan University, Shanghai 200433, China.

E-mail addresses: jyhuang@fudan.edu.cn (J. Huang), jphuang@fudan.edu.cn (J. Huang).

<http://dx.doi.org/10.1016/j.physb.2017.05.022>

Received 19 February 2017; Received in revised form 11 April 2017; Accepted 13 May 2017

Available online 16 May 2017

0921-4526/ © 2017 Elsevier B.V. All rights reserved.

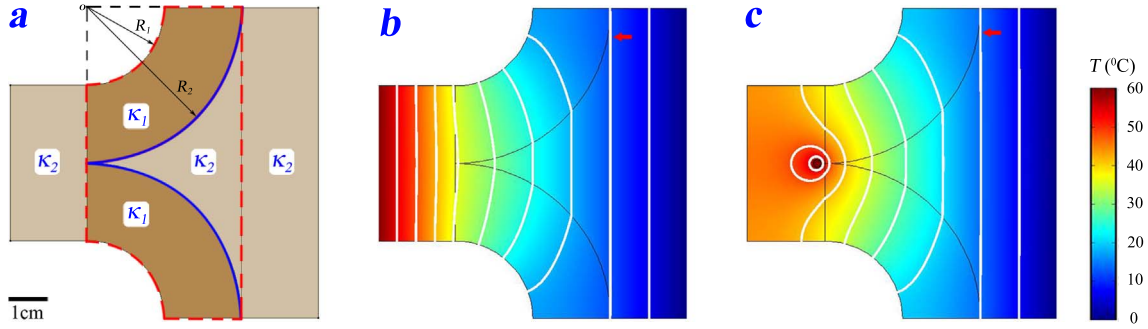


Fig. 1. (a) Schematic diagram of a thermal expander (area depicted by red dashed curves). Blue curves denote the boundaries between regions with thermal conductivities κ_1 and κ_2 (respectively). (b) Simulated expanding effect of thermal expander on a heat flow of line-shape front. (c) Simulated result of a heat flow of crooked front rectified to be of line-shape front by thermal expander. The point heat source is of diameter 2.2 mm. The black curves in (b) and (c) depict the structure and location of thermal expander. The white curves are isothermal lines (with steps of 6 °C for (b) and 6.9 °C for (c)) corresponding to the color legend. Each isothermal line arrowed describes the shape of flow front on the end-position of thermal expander. (For interpretation of the references to color in this figure legend, the reader is referred to the web version of this article.)

where, T is the temperature distributions in the space. Since the upper and lower parts of the thermal expander are symmetric, the general solutions can be obtained as

$$T_i = \sum_{n=1}^{\infty} [A_{2n-1}^i r^{2n-1} + B_{2n-1}^i r^{-(2n-1)}] \cos(2n-1)\theta, \quad (2)$$

where, A_{2n-1}^i and B_{2n-1}^i are constants determined by the boundary conditions, and T_i is the temperature potential in different regions ($i = 1, 2$). As to the thermal expander shown in Fig. 1a, $i = 1$ denotes the quarter ring areas ($R_1 < r < R_2$), and $i = 2$ denotes the connection area ($r > R_2$). Taking account of the continuities of the temperature potential and heat flow across the different interfaces, the boundary conditions are listed as

$$\begin{aligned} T_1|_{r=R_2} &= T_2|_{r=R_2}, \\ \kappa_1 \frac{\partial T_1}{\partial r} \Big|_{r=R_2} &= \kappa_2 \frac{\partial T_2}{\partial r} \Big|_{r=R_2}, \\ \kappa_1 \frac{\partial T_1}{\partial r} \Big|_{r=R_1} &= 0. \end{aligned} \quad (3)$$

Moreover, without being specified, the outer boundaries of the whole system are all set as insulated.

In order to eliminate the distortion caused by the shape of the device, only the first order factors in solutions are valid and we also must ensure $B_1^2 = 0$. Thus the required relationship of conductivities and shape parameters is finally derived to be

$$\frac{\kappa_1}{\kappa_2} = \frac{R_2^2 + R_1^2}{R_2^2 - R_1^2}. \quad (4)$$

For further discussion, the material of extension background (areas outside the red dashed lines) is also chosen to be Material II of κ_2 for simplicity.

3. Simulation and experiment

In this study, the Material I in the areas of two quarter rings is chosen to be Copper with thermal conductivity of $400 \text{ W} \cdot (\text{m} \cdot \text{K})^{-1}$. The inner and outer radiuses are set to be $R_1 = 2 \text{ cm}$ and $R_2 = 4 \text{ cm}$, respectively. Then the thermal conductivity κ_2 of Material II in the connection and extension areas is calculated from Eq. (4) to be $240 \text{ W} \cdot (\text{m} \cdot \text{K})^{-1}$.

Fig. 1b performs the simulated (Comsol) expanding effect of the thermal expander on a heat flow of line-shape front. The front of heat flow keeps line-shape in the connection area and also on the end-position of thermal expander, which verifies that the Eq. (4) is valid.

Interestingly, the simulation shown in Fig. 1c infers that the thermal expander could also efficiently rectify a crooked heat flow to be a line-shape one. As the crooked heat flow is from a point heat

source, Fig. 1c also indicates that the thermal expander could act as a point-to-line heat source converter.

For experimental demonstration of the thermal expander, the samples are fabricated on a homogeneous copper plate with thickness 0.1 mm. To obtain the thermal conductivity κ_2 of Material II, the effective medium approach [30] is adopted. As shown in Fig. 2, holes filled with Polydimethylsiloxane (PDMS) are hexagonally placed in the area of Material II with a lattice constant 4 mm. The corresponding thermal conductivity of PDMS is $0.15 \text{ W} \cdot (\text{m} \cdot \text{K})^{-1}$. The holes are achieved through wet-etching method [31]. The volume fraction f of hole is calculated from the Bruggeman formula [32].

$$(1-f) \frac{\kappa_{Cu} - \kappa_2}{\kappa_{Cu} + 2\kappa_2} + f \frac{\kappa_{PDMS} - \kappa_2}{\kappa_{PDMS} - 2\kappa_2} = 0. \quad (5)$$

Then the diameter of each hole is realized to be 2.2 mm.

A thin film (about 0.1 mm thick) PDMS is also deposited on the surface of each sample to reduce the heat conduction and convection by air [16]. This PDMS film could also minimize the influence of high reflection by copper surface on the experimental observation [16]. The thermal distribution of each sample is then observed through a FlirE60 infrared camera. For comparison, a referenced samples is also fabricated by replacing the thermal expander with a copper plate, while the extension background is kept the same. Illustrations for the referenced sample could be found in Fig. 3b.

The expanding effects of these designed samples are first verified by simulation. Results are shown in Figs. 3a and 3b. For experiments, the

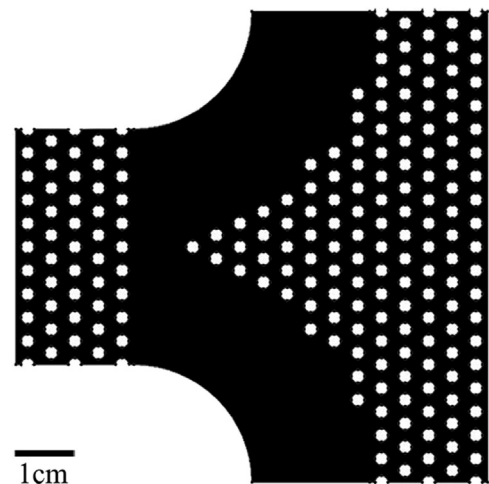


Fig. 2. Blueprint of the designed thermal expander for experiment. The black regions are copper and the white regions are PDMS with thermal conductivities of 400 and $0.15 \text{ W} \cdot (\text{m} \cdot \text{K})^{-1}$, respectively. The white holes are of diameter 2.2 mm and hexagonally placed with a lattice constant 4 mm.

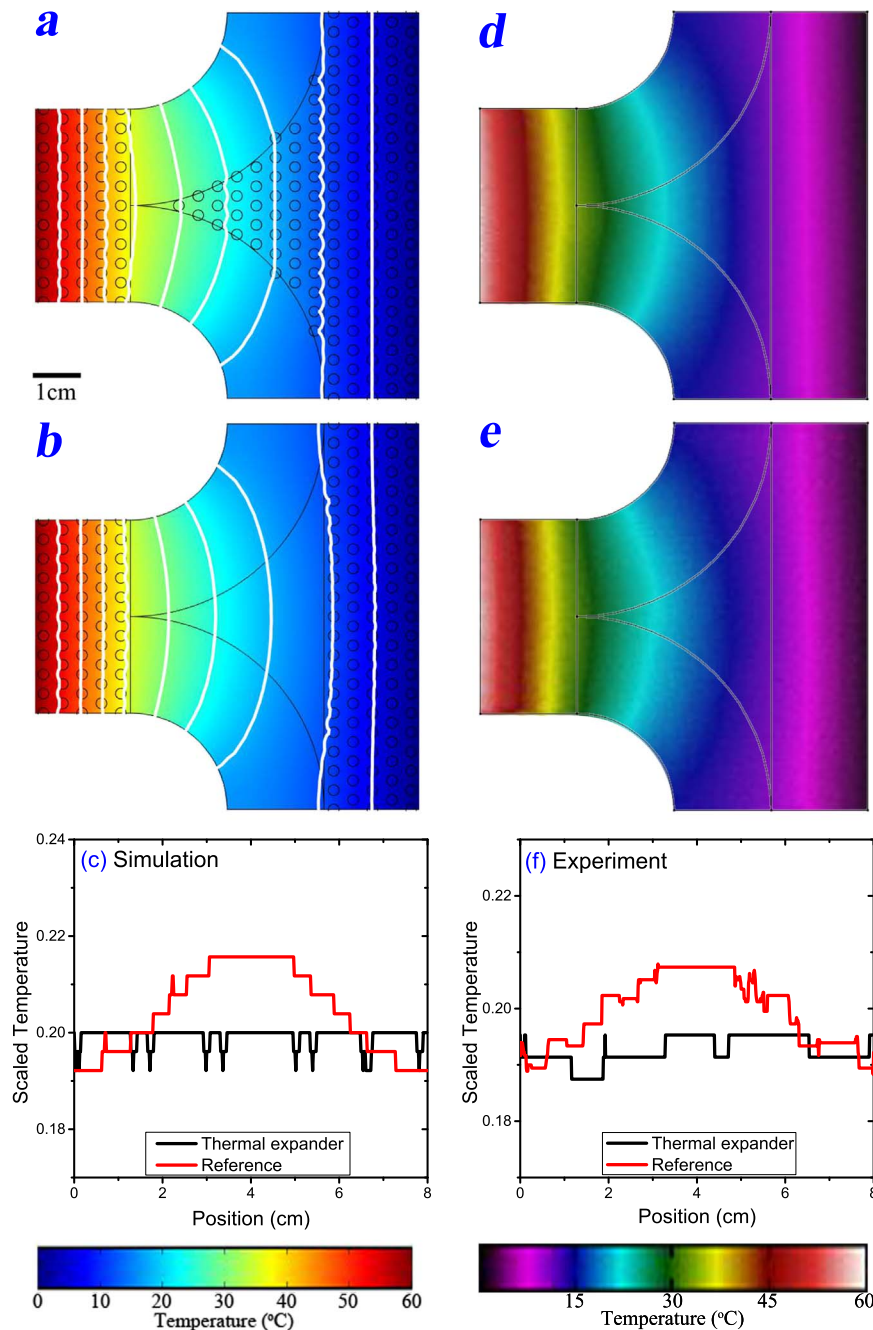


Fig. 3. Simulated expanding effects of (a) the designed thermal expander and (b) the referenced Copper sample. The corresponding results of experiments are shown in (d) and (e), respectively. The black curves depict the structure and location of the thermal expander for reference. The white curves in (a) and (b) are isothermal lines (with step of 6 °C) corresponding to the color legend. (c) and (f) perform the thermal distributions on the end-positions of each sample. The temperatures are all scaled by the temperature of heat source. The small fluctuation in each thermal curve is caused by the hole. (For interpretation of the references to color in this figure legend, the reader is referred to the web version of this article.)

heat flow of line-shape front is achieved by two water tanks. One water tank is heated and fixed at 60 °C, while the other tank is filled with ice water (0 °C). Results are exhibited in Figs. 3d and 3e.

The thermal distribution shown in Fig. 3d, with reference to that shown in Fig. 3a, clearly exhibits the experimental demonstration for the designed thermal expander. But the thermal distributions shown in Figs. 3b and 3e indicate that the line-shape flow front is distorted to be crooked when the line-shape heat flow passes through the referenced sample.

For a further comparison, the thermal distributions on the end-positions of each sample are exhibited in Figs. 3c (simulation) and 3f (experiment). Although the referenced sample is of higher temperature

distribution, we could observe that only the thermal distribution on the end-position of thermal expander is line-shape. This indicates that the thermal expander performs a more efficient way to expand the heat flow. Furthermore, the heat flow keeps line-shape in the connection area, which infers that the thermal expander also shows an advantage in extending the utilization area in practice.

To experimentally demonstrate the point-to-line conversion effect exhibited in Fig. 1c, the point heat source is achieved by a stainless steel cylinder with a cross section diameter 2.2 mm. Part of the cylinder is immersed into the heat water tank, while the tip of another part contacts to each sample on the position as shown in Fig. 4. The temperature of the tip is also controlled to be 60 °C. With the tank filled

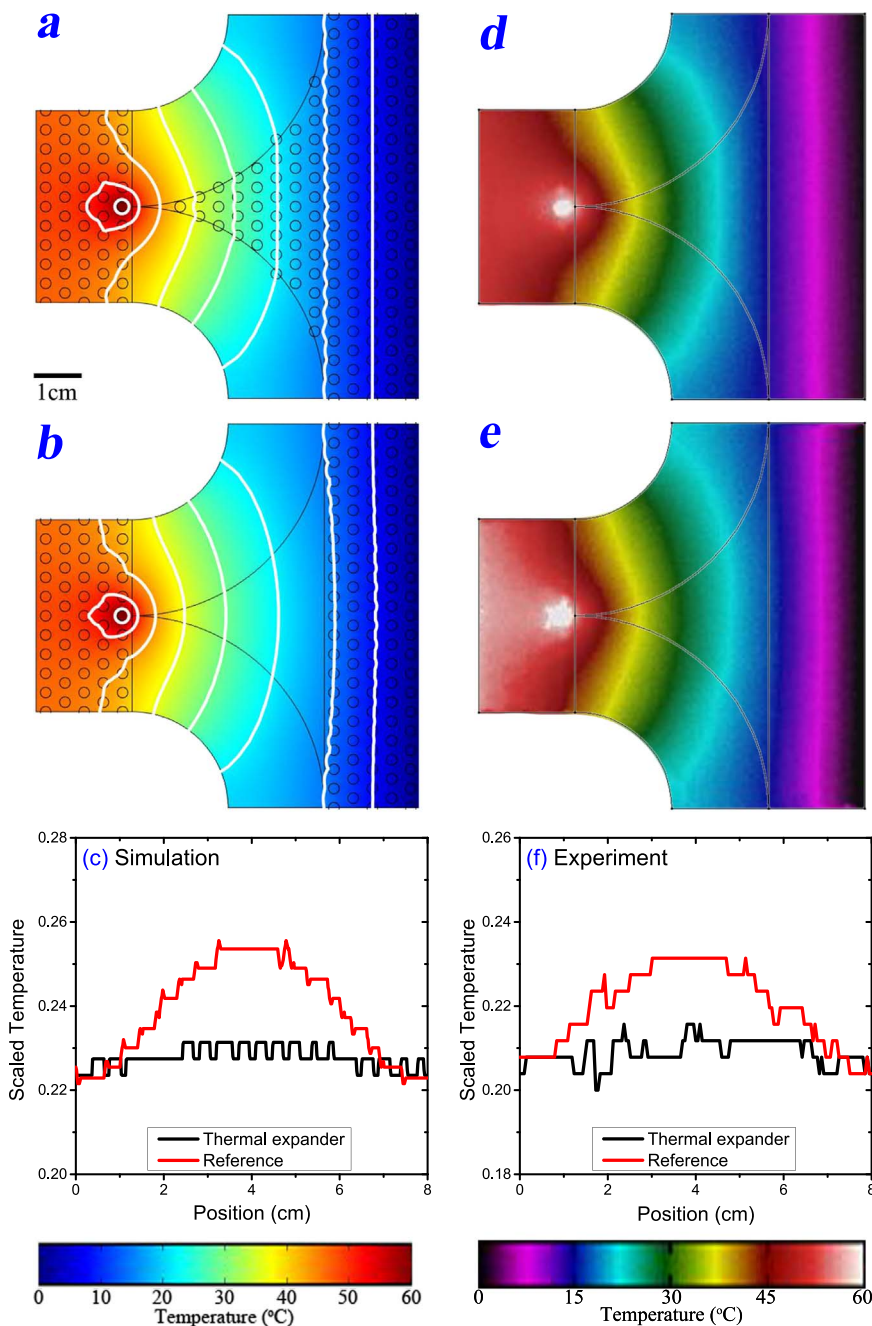


Fig. 4. Simulated thermal distributions of (a) the designed thermal expander and (b) the referenced Copper sample in point-line heat fields. The corresponding results of experiments are shown in (d) and (e), respectively. The black curves depict the structure and location of the thermal expander for reference. The white curves in (a) and (b) are isothermal lines (with steps of 7.3 °C) corresponding to the color legend. (c) and (f) perform the thermal distributions on the end-positions of each sample. The temperatures are all scaled by the temperature of heat source. The small fluctuation in each thermal curve is caused by the hole. (For interpretation of the references to color in this figure legend, the reader is referred to the web version of this article.)

with ice water, a point-line heat field is constructed. Results of experimental observations are shown in Fig. 4. For comparisons, the corresponding simulated results are also exhibited.

As to the designed thermal expander (Figs. 4a and 4d), the crooked front of heat flow is quickly rectified to be of line-shape front even in the connection area. But as to the referenced sample, the flow front are still crooked even far away from the end-point of the sample. A more clear comparison between the thermal distribution on the end-positions of each sample is exhibited in Figs. 4c (simulation) and 4f (experiment). Fig. 4 indicates that the thermal expander performs a more efficient way to rectify heat flow from crooked front to line-shape front. That is, the thermal expander performs a more efficient point-to-line heat source conversion.

4. Conclusion and perspectives

In conclusion, a two-component thermal expander is proposed and demonstrated through both simulation and experiment. The thermal expander performs an efficient way to expand a heat flow of line-shape front. Moreover, the thermal expander shows an advantage in rectifying a heat flow from crooked front to line-shape front. These properties make the thermal expander be an efficient device to convert a small-scale line or point heat source to a large-scale line heat source.

Currently, a large-scale heat flow of line-shape front is usually realized by a much larger scale heat source in practice [12,15,16]. But if the temperature of heat source is very high, obviously, the larger the heat source is, the higher risk we face. It is apparent that this risk can

be lowered by applying thermal expander. Furthermore, when the thermal industry is well established in the future [4], we suggest the thermal expander would have deep implication in thermal circuit to rectify and expand the heat flow.

Finally, since the electric and heat transfer all obey the Laplacian form, the derivation for dc case is the same as the thermal case; and finally we could achieve a equation similar with Eq. (4) by replacing each thermal conductivity with electric conductivity [19]. This implies that this two-component device could also work for dc case.

Acknowledgments

We thank Guoxi Nie and Yixuan Chen for their fruitful helps and discussion. This work is supported by the National Natural Science Foundation of China under Grant No. 11222544, by the Fok Ying Tung Education Foundation under Grant No. 131008, by the Program for New Century Excellent Talents in University (NCET-12-0121), and by the CNKBRS Funder Grant No. 2011CB922004.

References

- [1] C. Kittel, *Introduction of Solid State Physics*, 7th ed., John Wiley & Sons, New York, 2004.
- [2] L. Wang, B. Li, *Phys. Rev. Lett.* 99 (2007) 177208.
- [3] L. Wang, B. Li, *Phys. Rev. Lett.* 101 (2008) 267203.
- [4] N. Li, J. Ren, L. Wang, G. Zhang, P. Hanggi, B. Li, *Rev. Mod. Phys.* 84 (2012) 1045.
- [5] M. Maldovan, *Nat. (Lond.)* 503 (2013) 209.
- [6] C.W. Chang, D. Okawa, A. Majumdar, A. Zettl, *Science* 314 (2006) 1121.
- [7] M. Terraneo, M. Peyrard, G. Casati, *Phys. Rev. Lett.* 88 (2002) 094302.
- [8] B. Li, L. Wang, G. Casati, *Phys. Rev. Lett.* 93 (2004) 184301.
- [9] Z. Chen, C. Wong, S. Lubner, S. Yee, J. Miller, W. Jang, C. Hardin, A. Fong, J.E. Garay, C. Dames, *Nat. Commun.* 5 (2014) 5446.
- [10] A. Fornieri, M.J. Martínez-Pérez, F. Giazotto, *Appl. Phys. Lett.* 104 (2014) 183108.
- [11] M.J. Martínez-Pérez, A. Fornieri, F. Giazotto, *Nat. Nanotechnol.* 10 (2015) 303.
- [12] Y. Li, X. Shen, Z. Wu, J. Huang, Y. Chen, Y. Ni, J. Huang, *Phys. Rev. Lett.* 115 (2015) 195503.
- [13] C.Z. Fan, Y. Gao, J.P. Huang, *Appl. Phys. Lett.* 92 (2008) 251907.
- [14] J.Y. Li, Y. Gao, J.P. Huang, *J. Appl. Phys.* 108 (2010) 074504.
- [15] S. Narayana, Y. Sato, *Phys. Rev. Lett.* 108 (2012) 214303.
- [16] R. Schittny, M. Kadic, S. Guenneau, M. Wegener, *Phys. Rev. Lett.* 110 (2013) 195901.
- [17] H. Xu, X. Shi, F. Gao, H. Sun, B. Zhang, *Phys. Rev. Lett.* 112 (2014) 054301.
- [18] T. Han, X. Bai, D. Gao, J.T.L. Thong, B. Li, C.-W. Qiu, *Phys. Rev. Lett.* 112 (2014) 054302.
- [19] Y. Ma, Y. Liu, M. Raza, Y. Wang, S. He, *Phys. Rev. Lett.* 113 (2014) 205501.
- [20] T. Han, X. Bai, J.T.L. Thong, B. Li, C.-W. Qiu, *Adv. Mater.* 26 (2014) 1731.
- [21] Y. Gao, J.P. Huang, *EPL* 104 (2013) 44001.
- [22] X.Y. Shen, J.P. Huang, *Int. J. Heat. Mass Tranf.* 78 (2014) 1.
- [23] T. Han, T. Yuan, B. Li, C.-W. Qiu, *Sci. Rep.* 3 (2013) 01593.
- [24] F. Giazotto, M.J. Martínez-Pérez, *Nat. (Lond.)* 492 (2012) 401.
- [25] M.J. Martínez-Pérez, F. Giazotto, *Nat. Commun.* 5 (2014) 3579.
- [26] N.Q. Zhu, X.Y. Shen, J.P. Huang, *AIP Adv.* 5 (2015) 053401.
- [27] X.Y. Shen, Y.X. Chen, J.P. Huang, *Commun. Theor. Phys.* 65 (2016) 375.
- [28] T. Han, J. Zhao, T. Yuan, D.Y. Lei, B. Li, C.-W. Qiu, *Energy Environ. Sci.* 6 (2013) 3537.
- [29] T. Han, X. Bai, D. Liu, D. Gao, B. Li, J.T.L. Thong, C.-W. Qiu, *Sci. Rep.* 5 (2015) 10242.
- [30] J.P. Huang, K.W. Yu, *Phys. Rep.* 431 (2006) 87.
- [31] S. Franssila, *Introduction to Microfabrication*, 2nd ed, John Wiley & Sons, New York, 2010.
- [32] D.A.G. Bruggeman, *Ann. Phys. (Leipz.)* 24 (1935) 636.